Endoscopy in the Paul Trap: Measurement of the Vibratory Quantum State of a Single Ion

P. J. Bardroff, C. Leichtle, G. Schrade, and W. P. Schleich*
Abteilung für Quantenphysik, Universität Ulm, D-89069 Ulm, Germany
(Received 25 April 1996)

We reconstruct the density operator of the center-of-mass motion of an ion stored in a Paul trap by mapping the dynamics of the motion onto the internal dynamics of the ion. Our technique takes into account the explicit time dependence of the trap potential, operates outside the Lamb-Dicke limit, and is not restricted to pure states. We demonstrate the feasibility of this method using the example of a damped Schrödinger cat state. [S0031-9007(96)01127-1]

PACS numbers: 32.80.Pj, 03.65.Bz, 42.50.Vk

The recent experimental generation [1,2] of nonclassical states of the motion of an ion in a Paul trap [3] has propelled the field of quantum state preparation [4,5] into a new era. But how can we prove that the ion is indeed in a Fock, a squeezed, or a Schrödinger cat state? How can we measure a motional state which, due to the explicit time dependence of the binding force of the Paul trap, displays [6] a complicated time dependence? In this Letter we present the first method [7] that measures a vibratory state of an ion taking into account the complete time dependence of the Paul trap. Moreover, our technique operates outside the Lamb-Dicke regime [8] and is not limited to pure states only.

The central idea of our approach is to map the dynamics of the center-of-mass motion onto the internal degrees of the ion. The dynamics of the latter we can read out using quantum jumps [9]. Three techniques make this approach possible: (i) the well-known Floquet solution [10] of the harmonic oscillator with time-dependent frequency, (ii) the rotating wave approximation [11] resulting in a time independent s-phonon Jaynes-Cummings interaction Hamiltonian between the center-of-mass motion and the internal states of the ion [12], and (iii) the application of quantum state endoscopy [13,14] originally devised for the measurement of a field state to the problem at hand. We demonstrate the feasibility of Paul trap endoscopy using the example of a damped Schrödinger cat state.

We start from the Hamiltonian

$$\hat{H}(t) = \hat{H}_a + \hat{H}_{\rm cm}(t) + \hat{H}_{\rm int}(t) \tag{1}$$

of a single two-level ion moving along one direction in a Paul trap and interacting with a classical laser field, where $\hat{H}_a = \frac{1}{2}\hbar\omega_a\hat{\sigma}_z$ describes the two internal states with transition frequency ω_a and $\hat{\sigma}_z$ is the Pauli matrix.

The one-dimensional center-of-mass motion of an ion with mass m in a harmonic potential with time-dependent steepness

$$\omega^2(t) = \tfrac{1}{4}\,\omega_{\rm rf}^2[a + 2q\cos(\omega_{\rm rf}t)] \tag{2}$$

follows from the Hamiltonian

$$\hat{H}_{\rm cm}(t) = \tfrac{1}{2m}\,\hat{p}^2 + \tfrac{1}{2}\,m\omega^2(t)\hat{x}^2\,. \tag{3}$$

The dimensionless parameters a and q are proportional [3] to the dc and ac voltages applied to the trap, respectively, and $\omega_{\rm rf} \equiv 2\pi/T$ is the frequency of the ac voltage.

In the rotating wave approximation we model the interaction of the classical laser field with the two levels of the ion by the Hamiltonian [15]

$$\hat{H}_{\rm int}(t) = \hbar g\{\hat{\sigma}^+ \exp[-i(\omega_L t - k\hat{x})] + \text{H.c.}\}, \tag{4}$$

where g and k denote the interaction strength and the wave vector of the light field with frequency ω_L, respectively. The Pauli matrix $\hat{\sigma}^+$ is the raising operator for the internal levels of the ion. Hence the laser field couples the center-of-mass motion to the internal states.

In order to solve the Schrödinger equation $i\hbar|\dot{\Psi}\rangle = \hat{H}(t)|\Psi\rangle$ for the state vector $|\Psi(t)\rangle$ describing both the internal states and the center-of-mass motion it is convenient to work in the interaction picture. We recall the relation [16]

$$\tilde{\hat{x}}(t) \equiv \hat{U}_{\rm cm}^\dagger(t)\hat{x}\hat{U}_{\rm cm}(t) = \sqrt{\tfrac{\hbar}{2m\omega_r}}\,[\epsilon^*(t)\hat{b} + \epsilon(t)\hat{b}^\dagger], \tag{5}$$

where $\hat{U}_{\rm cm}(t) = \hat{T}\exp[-\frac{i}{\hbar}\int_0^t dt'\hat{H}_{\rm cm}(t')]$ is the propagator of the center-of-mass motion, $\hat{T}$ is the time-ordering operator, and operators with a tilde are in the interaction picture. We denote the annihilation and creation operators of a time independent reference harmonic oscillator [10,17] with frequency ω_r by $\hat{b}$ and $\hat{b}^\dagger$. Note that the reference frequency ω_r is an arbitrary real parameter, which we choose later in a convenient way. The complex function $\epsilon(t)$ satisfies the classical Mathieu differential equation

$$\ddot{\epsilon}(t) + \omega^2(t)\,\epsilon(t) = 0 \tag{6}$$

with the initial conditions $\epsilon(0) = 1$ and $\dot{\epsilon}(0) = i\,\omega_r$.

To bring out most clearly that the laser field induces transitions between the energy eigenstates $|n\rangle$ of the time-independent reference oscillator we express the center-of-mass motion part of the interaction Hamiltonian equation (4) in these states. Indeed the interaction Hamiltonian

$$\tilde{\hat{H}}_{\rm int}(t) = \sum_{n=0}^{\infty}\sum_{s=-n}^{\infty}\hbar\Omega^{(n,n+s)}(t)\hat{\sigma}^+|n\rangle\langle n+s| + \text{H.c.} \tag{7}$$

 0031-9007/96/77(11)/2198(4)$10.00

in the interaction picture involves all possible s-phonon transitions [12]. The time-dependent frequencies $\Omega^{(n,n+s)}(t) \equiv g e^{-i\Delta t}\langle n|\hat{D}[\alpha(t)]|n+s\rangle$ follow from Eq. (4) with the help of Eq. (5). They involve the matrix elements of the displacement operator $\hat{D}(\alpha) \equiv \exp(\alpha\hat{b}^\dagger - \alpha^*\hat{b})$ at the complex valued time-dependent displacement $\alpha(t) \equiv i\eta\epsilon(t)$, where $\eta \equiv k[\hbar/(2m\omega_r)]^{1/2}$ denotes the Lamb-Dicke parameter. Here $\Delta \equiv \omega_L - \omega_a$ is the detuning between the laser frequency and the atomic transition frequency. When we evaluate [18] the matrix element $\langle n|\hat{D}[\alpha(t)]|n+s\rangle$ the frequencies $\Omega^{(n,n+s)}(t)$ read for $s \geq 0$

$$\Omega^{(n,n+s)}(t) = g\left[\frac{n!}{(n+s)!}\right]^{1/2} \exp(-i\Delta t)[i\eta\epsilon^*(t)]^s \times \exp\left[-\frac{\eta^2}{2}|\epsilon(t)|^2\right] L_n^s(\eta^2|\epsilon(t)|^2). \quad (8)$$

Here L_n^s denotes the generalized Laguerre polynomial. Similar relations hold for $s < 0$.

We note that the time dependence of $\Omega^{(n,n+s)}(t)$ results from the detuning Δ and the complex valued function $\epsilon(t)$. In order to simplify this time dependence and hence the interaction Hamiltonian equation (7) we focus on the so-called Floquet solution

$$\epsilon^{(F)}(t) = \exp(i\mu t)\phi(t). \quad (9)$$

Here the characteristic exponent μ and the periodic function

$$\phi(t) = \phi(t+T) = \sum_{n=-\infty}^{\infty} c_n \exp(in\omega_{\rm rf}t) \quad (10)$$

are determined [10] by the trap parameters a and q. In the stable region of the Mathieu equation [19] the expansion coefficients c_n and the characteristic exponent μ are purely real. Then the frequency μ gives the secular frequency of the motion of the ion. Note that it is the specific choice [10]

$$\omega_r^{(F)} = \mu + \omega_{\rm rf}\sum_{n=-\infty}^{\infty} n c_n \quad (11)$$

of the reference frequency ω_r as the initial condition $\dot{\epsilon}(0) = i\omega_r^{(F)}$, which enforces the quasiperiodic solution Eq. (9) of the differential equation (6).

We substitute the Floquet solution $\epsilon^{(F)}(t)$, Eq. (9), into the time-dependent frequencies Eq. (8) and arrive at

$$\Omega^{(n,n+s)}(t) = \sum_{l=-\infty}^{\infty} \omega_l^{(n,n+s)} \exp[i(l\omega_{\rm rf} - s\mu - \Delta)t],$$

where the coefficients

$$\omega_l^{(n,n+s)} \equiv g\left[\frac{n!}{(n+s)!}\right]^{1/2}(i\eta)^s \times \int_{-T/2}^{T/2}\frac{dt}{T}[\phi^*(t)]^s e^{-\eta^2|\phi(t)|^2/2} \times L_n^s(\eta^2|\phi(t)|^2)e^{-il\omega_{\rm rf}t} \quad (12)$$

follow by expanding the part of $\Omega^{(n,n+s)}$ in Fourier series, which is periodic in $T = 2\pi/\omega_{\rm rf}$. When we now use this expression for $\Omega^{(n,n+s)}$ the interaction Hamiltonian in the interaction picture reads

$$\hat{\tilde{H}}_{\rm int}(t) = \sum_{n=0}^{\infty}\sum_{s=-n}^{\infty}\sum_{l=-\infty}^{\infty}\hbar\omega_l^{(n,n+s)} \times \exp[i(l\omega_{\rm rf} - s\mu - \Delta)t] \times \hat{\sigma}^+|n\rangle\langle n+s| + \text{H.c.} \quad (13)$$

We emphasize that this representation is exact. It shows that the time dependence of $\hat{\tilde{H}}_{\rm int}(t)$ is governed by the specific combination $l\omega_{\rm rf} - s\mu - \Delta$ of all harmonics of the frequency $\omega_{\rm rf}$ and of the secular frequency μ, and the detuning Δ. This feature allows us to perform a time average [11] of $\hat{\tilde{H}}_{\rm int}(t)$ in order to obtain an s_0-phonon Hamiltonian as we show now.

So far we have not yet specified the detuning Δ. We choose it in such a way that one of the terms in the sums in Eq. (13) is slowly varying, whereas all the others are rapidly oscillating. This happens when $s_0\mu + \Delta \equiv l_0\omega_{\rm rf}$. Note that this condition leads to an interesting number theoretical problem. In order to achieve a large coupling to the field we choose Δ such that only the term with the largest coefficient $\omega_{l_0}^{(n,n+s_0)}$ survives the time averaging for s_0 fixed. Hence we choose $\Delta = l_0\omega_{\rm rf} - s_0\mu$ provided that $\Delta + s\mu$ is not a multiple integer of the frequency $\omega_{\rm rf}$ for all $s \neq s_0$. With the help of the rotating wave approximation we therefore arrive at the time averaged Hamiltonian

$$\hat{\tilde{H}}_{\rm int} = \sum_{n=0}^{\infty}\hbar\omega_{l_0}^{(n,n+s_0)}\hat{\sigma}^+|n\rangle\langle n+s_0| + \text{H.c.}, \quad (14)$$

which is the s_0-phonon Jaynes-Cummings Hamiltonian.

Since we face the Jaynes-Cummings Hamiltonian, we can use the method of quantum state endoscopy [13,14] and reconstruct the initial vibrational density operator $\hat{\rho}(0)$ of the ion from the measured time evolution of its internal state. For the application of this method we use the coherent superposition $|\Psi_a\rangle = (|e\rangle + e^{i\varphi}|g\rangle)/\sqrt{2}$ of the excited and the ground state as initial internal state. We then can extract from the probability

$$\begin{aligned} P_e(t;\varphi) &\equiv \text{Tr}_{\rm cm}\langle e|e^{-i\hat{\tilde{H}}_{\rm int}t/\hbar}[\hat{\rho}(0)\otimes|\Psi_a\rangle\langle\Psi_a|]e^{i\hat{\tilde{H}}_{\rm int}t/\hbar}|e\rangle \\ &= \tfrac{1}{2} - \tfrac{1}{4}\sum_{n=0}^{s_0-1}\rho_{n,n} \\ &\quad + \tfrac{1}{4}\sum_{n=0}^{\infty}\cos(2\omega_{l_0}^{(n,n+s_0)}t)(\rho_{n,n} - \rho_{n+s_0,n+s_0}) \\ &\quad - \tfrac{1}{2}\sum_{n=0}^{\infty}\sin(2\omega_{l_0}^{(n,n+s_0)}t)\text{Im}[(-i)^{s_0}\rho_{n,n+s_0}e^{-i\varphi}] \end{aligned}$$

of finding the ion in the excited state $|e\rangle$ the matrix elements $\rho_{n,n+s_0} = \langle n|\hat{\rho}(0)|n+s_0\rangle$ of the density operator of the center-of-mass motion. Following Ref. [14], we measure the internal dynamics, that is, $P_e(t;\varphi)$, for two different phases φ, N interaction times, and $s_{\rm max}$ detunings. Here N and $s_{\rm max}$ denote the dimensions over which

the density matrix has significant elements. The algorithm of Ref. [14] then allows us to reconstruct from these data the full density matrix.

We demonstrate the feasibility of the reconstruction scheme using as the initial center-of-mass density operator $\hat{\rho}(0)$ a damped Schrödinger cat state

$$\hat{\rho}(0) = p\,\hat{\rho}_{\mathrm{incoh}}(\alpha) + (1 - p)\hat{\rho}_{\mathrm{cat}}(\alpha). \qquad (15)$$

Here p is a weight factor,

$$\hat{\rho}_{\mathrm{incoh}}(\alpha) = \tfrac{1}{2}[|\alpha\rangle\langle\alpha| + |-\alpha\rangle\langle-\alpha|]$$

is a incoherent superposition of two coherent states, and

$$\hat{\rho}_{\mathrm{cat}}(\alpha) = \tfrac{|\mathcal{N}|^2}{2}[|\alpha\rangle - |-\alpha\rangle][\langle\alpha| - \langle-\alpha|]$$

is a Schrödinger cat state with normalization constant $\mathcal{N}$. Note that we have chosen the coherent state $|\alpha\rangle$ with respect to the time-independent reference oscillator with frequency $\omega_r^{(F)}$. We emphasize that Ref. [2] reported the birth of Schrödinger cats of this kind.

For the numerical simulation of Paul trap endoscopy we use the parameters $p = 0.5$ and $\alpha = 1.5$. Since in this case the Schrödinger cat lies on the real axis, the matrix elements $\rho_{n,m}$ are real. Moreover, we take the trap parameters $a = 0$, $q = 0.4$, and $\eta = 1$. In order to simulate experimental uncertainties in a simple way and to test the stability of the reconstruction procedure, we round the calculated values of $P_e(t;\varphi)$ to the precision of one-tenth.

In Fig. 1(a) we show the relevant matrix elements $\rho_{n,m}$ of the exact density operator Eq. (15). Note that the matrix elements of the reconstructed density operator $\hat{\rho}^{(r)}$ become complex. In Figs. 1(b) and 1(c) we show the real part and the imaginary part of its elements, respectively. We emphasize that there is an excellent agreement between the exact and reconstructed density matrix as is apparent from Figs. 1(c) and 1(d) where we show the difference between the exact and the reconstructed matrix elements in their imaginary and real parts.

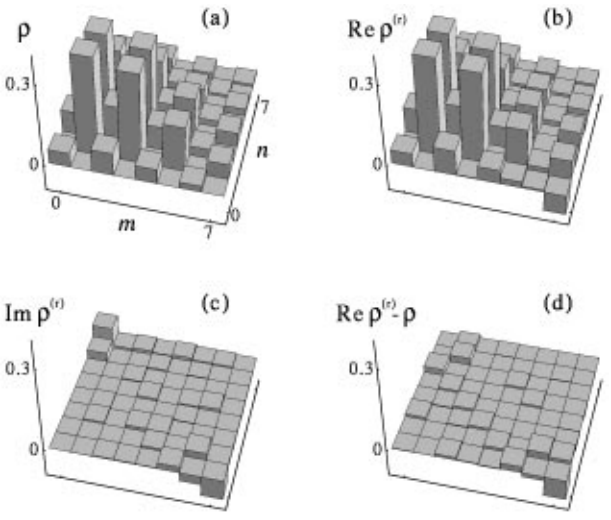

FIG. 1. Paul trap endoscopy illustrated by a damped Schrödinger cat. In (a) we show the matrix elements $\rho_{n,m}$ in energy representation of the cat to be reconstructed. All matrix elements are real. In (b) and (c) we display the real and imaginary parts of the reconstructed matrix elements $\rho_{n,m}^{(r)}$. The tiny differences between the two density matrices in their real and imaginary parts as shown in (d) and (c) demonstrate the feasibility of Paul trap endoscopy.

The present treatment takes into account the complete time dependence of the trap potential. To bring out the importance of this time dependence, we now compare our exact treatment to the effective potential approximation [15]. The latter describes the vibrational degree of freedom in the limit $a, q \to 0$ by an effective, time-independent harmonic oscillator with frequency μ. In this case, Eq. (10) simplifies to $\phi(t) \simeq 1$, and hence Eq. (9) reduces to $\epsilon^{(F)}(t) \simeq e^{i\mu t}$. As a consequence, the Rabi frequencies $\omega_l^{(n,n+s)}$ Eq. (12) all vanish except for $l \equiv 0$ which read [12]

$$\omega_{\mathrm{eff}}^{(n,n+s)} = g\left[\frac{n!}{(n+s)!}\right]^{1/2}(i\eta)^s e^{-\eta^2/2} L_n^s(\eta^2). \qquad (16)$$

In Fig. 2 we show the effective Rabi frequencies $\omega_{\mathrm{eff}}^{(n,n+1)}$ of the one-phonon transition by crosses and compare it to the exact frequencies $\omega_{l=0}^{(n,n+1)}$ for the trap parameters $a = 0$ and the three different values $q = 0.01$ (diamonds), $q = 0.2$ (triangles), and $q = 0.4$ (squares). These parameters are often used [1,2,20] in experiments. For this figure we have chosen the Lamb-Dicke parameter $\eta = 1$. To guide the eye we have connected the discrete values by continuous curves. Whereas for the small value $q = 0.01$ the frequencies almost coincide, we find considerable differences for the values $q = 0.2$ and 0.4. In these cases the differences between the exact and the effective Rabi frequencies are of the same order as the differences between neighboring Rabi

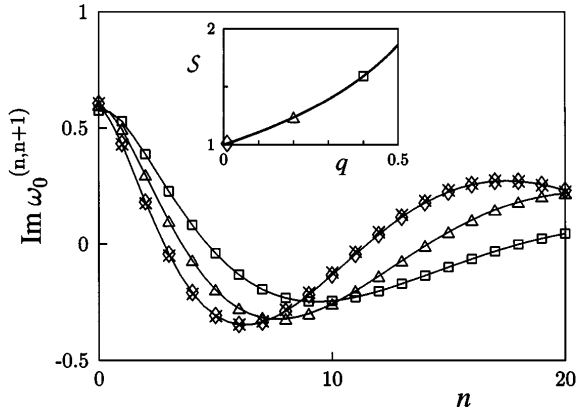

FIG. 2. Comparison between the Rabi frequencies $\omega_{\mathrm{eff}}^{(n,n+1)}$ within the effective potential approximation (crosses) and the exact frequencies $\omega_0^{(n,n+1)}$ including the micromotion for the trap parameters $a = 0$ and three different values of q. Note that according to Eqs. (12) and (16) these frequencies are purely imaginary. The diamonds correspond to $q = 0.01$, the triangles to $q = 0.2$, and the squares to $q = 0.4$. The inset shows the squeezing parameter S for $a = 0$ as a function of q.

frequencies. However, for reconstructing the density operator, it is crucial to distinguish neighboring Rabi frequencies. Hence the influence of the micromotion is not negligible for these values of q.

Another consequence of the effective potential approximation is that the states $|n\rangle$ represent now the energy eigenstates $|n\rangle_\mu$ of the static oscillator with frequency μ. The two different sets of basis states corresponding to the two oscillators with frequencies $\omega_r^{(F)}$ and μ are connected by the squeezing operation $\hat{S}(r) = \exp[r(\hat{b}^{\dagger 2} - \hat{b}^2)/2]$ characterized by the parameter r. It is the ratio $S = \mu/\omega_r^{(F)} = \exp(2r)$ which determines the magnitude of squeezing. In the inset of Fig. 2 we show this ratio as a function of q for $a = 0$. Again the diamond, triangle, and square correspond to the value for $q = 0.01$, 0.2, and 0.4, respectively.

We conclude by summarizing our main results. We have presented a technique that allows us to measure the quantum state of the center-of-mass motion of an ion moving in a Paul trap. In contrast to related work [7] our scheme takes the explicit time dependence of the Paul trap into account. This time dependence might also be relevant for the recent discussions on quantum gates [21] and the quantum computer [22] resulting from many ions stored in a linear trap. We note that our method operates outside of the Lamb-Dicke limit. Moreover, we emphasize that the method is not limited to pure states only. Using the example of a damped Schrödinger cat we have shown that it is possible to perform endoscopy in the Paul trap.

We thank I. Sh. Averbukh, S. L. Braunstein, I. Cirac, H. J. Kimble, R. L. de Matos Filho, O. V. Man'ko, V. I. Man'ko, W. Vogel, S. Wallentowitz, and P. Zoller for fruitful discussions. In particular, we thank D. Leibfried for sending us a preprint of Ref. [23]. We (P.J.B. and C.L.) gratefully acknowledge the support of the DFG.

Note added.—After the completion of this work we have learned that the Boulder group [23] has indeed measured the quantum state of the motion of an ion in a Paul trap.

*Also at Max-Planck-Institut für Quantenoptik, D-85748 Garching, Germany.

[1] D. M. Meekhof *et al.*, Phys. Rev. Lett. **76**, 1796 (1996).
[2] C. Monroe *et al.*, Science **272**, 1131 (1996).
[3] W. Paul, Rev. Mod. Phys. **62**, 531 (1990).
[4] For the preparation of field states, see K. Vogel *et al.*, Phys. Rev. Lett. **71**, 1816 (1993); A. S. Parkins *et al.*, Phys. Rev. Lett. **71**, 3095 (1993); C. K. Law and J. H. Eberly, Phys. Rev. Lett. **76**, 1055 (1996).
[5] For the preparation of states of the motion, see J. I. Cirac *et al.*, Phys. Rev. Lett. **70**, 556 (1993); J. I. Cirac *et al.*, Phys. Rev. Lett. **70**, 762 (1993); R. L. de Matos Filho and W. Vogel, Phys. Rev. Lett. **76**, 608 (1996).
[6] G. Schrade *et al.*, Quant. Semiclass. Opt. **7**, 307 (1995).
[7] For the measurement of the motional state in the time independent effective harmonic potential, see S. Wallentowitz and W. Vogel, Phys. Rev. Lett. **75**, 2932 (1995); J. F. Poyatos *et al.*, Phys. Rev. A **53**, R1966 (1996); C. D'Helon and G. J. Milburn, Phys. Rev. A **54**, R25 (1996).
[8] The Lamb-Dicke limit arises when the characteristic length of the quantum mechanical state of the motion is small compared to the wave length of the light field. See the original papers by W. E. Lamb, Phys. Rev. **51**, 187 (1937); R. H. Dicke, Phys. Rev. **89**, 472 (1953).
[9] W. Nagourney *et al.*, Phys. Rev. Lett. **56**, 2797 (1986); T. Sauter *et al.*, Phys. Rev. Lett. **57**, 1696 (1986); J. C. Bergquist *et al.*, Phys. Rev. Lett. **57**, 1699 (1986).
[10] R. J. Glauber, in *Laser Manipulation of Atoms and Ions*, Proceedings of the International School of Physics "Enrico Fermi," Course CXVIII (Varenna, July, 1992), edited by E. Arimondo *et al.* (North-Holland, Amsterdam, 1992).
[11] In the context of laser cooling, a similar time averaging was used by J. I. Cirac *et al.*, Phys. Rev. A **49**, 421 (1994). However, their analysis focused on the Lamb-Dicke limit only.
[12] W. Vogel and R. L. de Matos Filho, Phys. Rev. A **52**, 4214 (1995).
[13] W. Vogel *et al.*, J. Opt. Soc. Am. B **4**, 1633 (1987).
[14] P. J. Bardroff *et al.*, Phys. Rev. A **51**, 4963 (1995); P. J. Bardroff *et al.*, Phys. Rev. A **53**, 2736 (1996).
[15] C. A. Blockley *et al.*, Europhys. Lett. **17**, 509 (1992).
[16] See, for example, Ref. [11], Eq. (A2).
[17] V. V. Dodonov and V. I. Man'ko, in *Invariants and the Evolution of Nonstationary Quantum Systems*, edited by M. A. Markov (Novo Science, New York, 1989).
[18] K. E. Cahill and R. J. Glauber, Phys. Rev. **177**, 1857 (1969).
[19] M. Abramowitz and I. A. Stegun, *Handbook of Mathematical Functions* (Dover, New York, 1972).
[20] R. Blümel *et al.*, Phys. Rev. A **40**, 808 (1989).
[21] C. Monroe *et al.*, Phys. Rev. Lett. **75**, 4714 (1995).
[22] J. I. Cirac and P. Zoller, Phys. Rev. Lett. **74**, 4091 (1995).
[23] D. Leibfried *et al.* (to be published).